Computers and Chemical Engineering 63 (2014) 51–65

Contents lists available at ScienceDirect

Computers and Chemical Engineering

journal homepage: www.elsevier.com/locate/compchemeng

Fully compositional and thermal reservoir simulation

Rustem Zaydullin[a], Denis V. Voskov[a], Scott C. James[b], Heath Henley[c], Angelo Lucia[d,*]

[a] Department of Energy Resources Engineering, Stanford University, Stanford, CA, United States
[b] Exponent, Inc., 320 Goddard, Suite 200, Irvine, CA 92618, United States
[c] Department of Chemical Engineering, University of Rhode Island, Kingston, RI 02881, United States
[d] FlashPoint LLC, Narragansett, RI 02882, United States

ARTICLE INFO

Article history:
Received 18 April 2013
Received in revised form
16 December 2013
Accepted 22 December 2013
Available online 8 January 2014

Keywords:
Process systems engineering
Enhanced oil recovery
Steam injection
STRIP
Fully compositional
Thermal reservoir simulation

ABSTRACT

Fully compositional and thermal reservoir simulation capabilities are important in oil exploration and production. There are significant resources in existing wells and in heavy oil, oil sands, and deep-water reservoirs. This article has two main goals: (1) to clearly identify chemical engineering sub-problems within reservoir simulation that the PSE community can potentially make contributions to and (2) to describe a new computational framework for fully compositional and thermal reservoir simulation based on a combination of the Automatic Differentiation-General Purpose Research Simulator (AD-GPRS) and the multiphase equilibrium flash library (GFLASH). Numerical results for several chemical engineering sub-problems and reservoir simulations for two EOR applications are presented. Reservoir simulation results clearly show that the Solvent Thermal Resources Innovation Process (STRIP) outperforms conventional steam injection using two important metrics – sweep efficiency and oil recovery.

1. Introduction

Modeling and simulation to predict long-term performance of oil recovery methods (i.e., reservoir simulation) is a topic studied for over 50 years (see Douglas et al., 1959; Price & Coats, 1974; Todd et al., 1972). Early reservoir models (e.g., black-oil reservoir models) were typically based upon rigorous mass-balance equations for key species (oil, water, and gas), but only used approximate phase equilibria (e.g., no oil dissolved in the water phase) and/or neglected energy balances. By the 80's, reservoir simulation had reached a level of maturity to warrant the first Society of Petroleum Engineers (SPE) Comparative Solutions Project on 3-D Black Oil Reservoir Simulation (Odeh, 1981) in which seven different companies participated. To date, there have been ten separate comparative solution projects sponsored by the SPE with topics that include three-phase behavior, steam injection, horizontal wells, and effective grid-generation and up-scaling techniques. These Comparative Solutions Projects papers are useful for readers new to reservoir simulation or those simply interested in learning more about challenging issues in this area.

Today, reservoir simulation has reached a point where advanced concepts such as dual-porosity models, rigorous phase behavior, energy-balance considerations, fully implicit time stepping with Newton's method to solve the reservoir model equations at each time step, iterative linear solvers, finite difference, and/or analytical Jacobian matrices (to name a few) are available as modeling components.

There remains considerable oil in place (OIP) in many reservoirs that are either in current operation or have been shutdown (often with infrastructure remaining in place). There are also large amounts of fossil fuels in heavy oil, oil sands, and deep-sea reservoirs – but these hydrocarbons are more challenging and more costly to produce. An increase in production at a standard oil field of just 1% can represent a $25 B opportunity. Many oil producers are considering enhanced oil recovery (EOR) methods such as steam injection and in situ CO_2 + steam injection (i.e., Solvent Thermal Resource innovative Process or STRIP) as a means of increasing recovery. Modeling STRIP, and other advanced EOR methods necessarily requires both fully compositional and thermal reservoir flow simulation capabilities, something that remains challenging.

Perhaps it is not surprising that various aspects (or sub-problems) of fully compositional and thermal reservoir modeling and simulation are, in many ways, similar to modeling and equation-solving task associated with the kinds of chemical processes with which the process systems engineering (PSE) community and readership of Computers & Chemical Engineering are familiar. These sub-problems include

* Corresponding author. Tel.: +1 401 789 1546.
E-mail addresses: flashpoint_llc@verizon.net, lucia@egr.uri.edu (A. Lucia).

0098-1354/$ – see front matter © 2013 Elsevier Ltd. All rights reserved.
http://dx.doi.org/10.1016/j.compchemeng.2013.12.008

Nomenclature

a_{ij}	number of atoms j in molecule i
A_j	total amount of atom j
B_{oil}	oil surface-to-reservoir formation volume factor
c_1,c_2,c_3,c_4	coefficients of cubic EOS
$[c]$	equilibrium ion solubility limit
C	total number of components
$C_{p,i}$	ideal gas heat capacity for ith component
f_i	partial fugacity of component i in solution
F	total density
g	acceleration due to gravity
G	heat conduction flux
ΔG_f^0	standard Gibbs free energy of formation
H	enthalpy
ΔH_f^0	standard heat of formation
ΔH_R^0	standard heat of reaction
K,K^k	intrinsic rock or soil permeability, thermal conductivity
K_{sp}	equilibrium solubility product
k_{ij}	binary interaction parameters
M	mass source or sink term
MW	molecular weight
n,n_i	vector of mole numbers, ith component mole number
p,p_c	pressure, critical pressure
P	total number of phases
Q	energy source or sink term
Q_{sp}	ion solubility product
r	oxygen-to-methane ratio
R	universal gas constant, relative permeability
S	saturation or amount of salt precipitate
t	time
T,T_c,T_{jm}	absolute temperature, critical temperature, transmissibility coefficient
U	internal energy
V	volumetric flow, volume of grid block
x,x_i	vector of liquid phase mole fractions, ith component liquid mole fraction
z	coordinate in direction of gravity, compressibility factor, vector of feed compositions

Greek symbols

ϕ	porosity
φ_i,φ_M	partial fugacity coefficient of component i, mixture fugacity coefficient
Φ	geometric part of flux
γ	mass density at interface
η	sweep ratio
κ	permeability
λ	mobility
μ	viscosity, chemical potential
ρ	density

Superscripts

k	phase index
L	liquid
V	vapor
0	standard state

Subscripts

c	critical property
C	number of components
i	component or summation index
M	porous media

1. Multi-phase equilibrium or flash.
2. Chemical reaction equilibrium.
3. Combined chemical and phase equilibrium.
4. Adiabatic flame temperature determination.
5. Heat and mass transfer in porous media.
6. Models consisting of differential algebraic equations (DAEs).
7. Nonlinear equation-solving using Newton and trust region methods.
8. Iterative linear equations solving.

Thus it is our opinion that chemical engineers, particularly those in the process systems engineering (PSE) community, are in a unique position to make significant contributions to various aspects of reservoir simulation.

In this paper, we present an advanced reservoir modeling and simulation framework for fully compositional and thermal reservoir simulation and subsequently apply this simulation framework to a comparative study of steam injection and STRIP in EOR applications. We also identify those sub-problems to which the PSE community can contribute. Accordingly, this work is organized as follows. Section 2 gives an overview of the relevant literature. In Section 3, a generalized reservoir model is presented; it includes model equations for both the reservoir and the bulk-phase length scales. Coupling between the reservoir and other constitutive equations needed to close the model (e.g., multiphase equilibrium flash, viscosity correlations, Darcy's law, heat conduction, etc.) are also described. In Section 4, details that describe how model equations are formulated and solved at various computational levels are given. Specific algorithmic features of the coupled methodology are also presented. In Section 5, steam injection and STRIP are introduced along with common metrics used to evaluate thermal EOR techniques. In Section 6, several relevant sub-problems are presented and solved prior to the application of this new reservoir simulation framework to two reservoir examples that demonstrate modeling and simulation capabilities and quantify the reliability and computational efficiency of the approach. A quantitative comparison of steam injection and STRIP is provided for the first reservoir simulation example using common performance metrics. The second example compares the performance of a modified compositional space adaptive tabulation (CSAT) with the conventional multiphase flash approach. Finally, in Section 7 conclusions of this work are drawn and future needs are highlighted while in Section 8 some additional sub-problems of interest to the PSE community are identified.

2. Literature survey

The focus of this article is numerical reservoir simulation, which comprises a vast body of literature and thus it is not possible to survey all relevant scientific papers. Therefore in this section only a summary of those papers and numerical methods directly relevant to the modeling and simultaneous solution of numerical reservoir models is presented. We refer the reader to the book by Peaceman (2000) for an introduction to the fundamentals of reservoir modeling and simulation and a description of some of the foundational numerical methods that have been developed. A secondary focus of this manuscript is to identify sub-problems within a larger reservoir

simulation that are clearly within the skill set of process systems engineers.

Some of the earliest work in numerical reservoir simulation dates back to 1959 and the pioneering work of Douglas et al. (1959), who developed numerical methods for the simultaneous solution of time dependent two-phase flow problems in one and two spatial directions. Governing partial differential equations (PDEs) describing conservation of mass and flow were converted to nonlinear algebraic equations using difference approximations and the resulting nonlinear algebraic model equations were then solved using various numerical methods including alternating-directions implicit, Jacobi iteration, successive over-relaxation, Gauss-Seidel iteration, and other established techniques. We refer the reader to the book by Ortega and Rheinboldt (1970) for a comprehensive description of these numerical methods. The work of Douglas et al. (1959) was later extended to three spatial dimensions by Coats et al. (1967) and to three-phase flow problems by Peery and Herron (1969) and Sheffield (1969). Other journal articles that address additional physics in reservoir simulations and solve model equations simultaneously include those by Snyder (1969), Settari and Aziz (1974), and Trimble and McDonald (1976). Key differences among many of the early approaches to reservoir simulations reside largely in model formulation and the methods used to solve the resulting algebraic model equations. These differences persist today. Note that all of the topics just described are familiar to the PSE community – dynamical equations describing conservation of mass and energy, differencing, and nonlinear equation solving.

State-of-the-art reservoir simulation has moved to two basic nonlinear formulations – a natural formulation (Coats, 1980) and a molar formulation (Acs, 1985). Large sets or subsets of nonlinear algebraic equations result from discrete representations of the governing PDEs that describe the spatial and temporal evolution of the system. The most commonly used approaches for discrete representation are finite-difference or finite-volume approximations on structured or unstructured grids. The resulting algebraic equations are generally solved simultaneously using variants of Newton's method, although various forms of model reductions are also used. In the natural formulation, pressure, temperature, saturation, and all phase compositions for all grid blocks comprise the set of unknown variables. In the molar formulation, which is probably the formulation that is more familiar to engineers in the PSE community, pressure, temperature, and overall compositions (or total component mass) are the unknown variables. While there are many approaches to model formulation and solution, some of the more commonly used methods are differentiated by the temporal discretization scheme – Fully Implicit Method (FIM), IMplicit Pressure Explicit Saturation (IMPES), IMplicit Pressure and SATuration (IMPSAT), and Adaptive Implicit Methods (AIM).

For the description of different solution techniques that follows, we use the natural formulation in a reservoir application in which the pressures, saturations, and phase compositions for all grid blocks are the unknown variables. In the FIM, all pressures, saturations, and compositions of all phases are computed simultaneously at each time step. One of the key advantages of the FIM is that it is unconditionally stable. In contrast, the IMPES methodology treats all terms that depend on saturation and compositions, except the transient terms, as explicit functions of these variables. This allows saturation and composition to be decoupled from the pressure, resulting in a smaller subset of equations to be solved simultaneously, which reduces overall computational demand. However, because IMPES involves some explicit terms, integration may not be numerically stable in regions where volumetric flows are large. As a result, the computational time saved by reducing the size of the system of nonlinear equations can often be negated by smaller time stepping and, in the worst case, can lead to model failure. IMPSAT is similar IMPES, except that IMPSAT treats pressures and saturation variables for all grid blocks implicitly and phase compositions for all grid blocks explicitly. AIM, on the other hand, is intended to marry the best characteristics of FIM, IMPSAT, and IMPES by switching between different solution methods using one or more prescribed metrics, as solution stability demands. For example, AIM might use the spectral radius of a transformation matrix in the residuals of the mass conservation equations to decide when to switch from FIM in regions where instabilities in IMPES are likely, but use IMPES everywhere else (Cao, 2002). A good survey of the numerical characteristics of FIM, IMPES, and AIM is given by Marcondes et al. (2009). Regardless of the formulation, many current solution methods use some form of iterative linear equation solver (e.g., GMRES or other Krylov subspace methods) with pre-conditioning to solve the linear system of equations that determines the Newton correction to the variables at each time step.

3. Reservoir model equations

The equations describing the time evolution of fluid composition, temperature, and pressure in a reservoir comprise a set of coupled, nonlinear PDEs that describe conservation of mass, energy, and momentum. In addition, various thermo-physical properties, equilibrium (or non-equilibrium) behavior of fluid phases, properties of porous media, and well-configuration specifications are included as algebraic constraints to the governing PDEs. In this article, the governing PDEs are represented in discrete form using finite-volume discretization and, when used with additional constraints, they form a large set of nonlinear algebraic equations. In this section, the reservoir equations as well as other constitutive equations are described.

3.1. Reservoir model equations in general form

The nonlinear time-dependent PDEs that represent conservation of mass and energy in a reservoir are given by

$$\frac{\partial}{\partial t}\left(\phi\sum_{k=1}^{P}\rho^k x_i^k S^k\right)-\sum_{k=1}^{P}\left(\rho^k x_i^k V^k+S^k J_i^k\right)-Q_i=0,\quad i=1,\ldots,C \tag{1}$$

and

$$\frac{\partial}{\partial t}\left[(1-\phi)\rho_M U_M+\phi\sum_{k=1}^{P}\rho^k U^k S^k\right]-\sum_{k=1}^{P}\left(\rho^k H^k V^k+S^k G^k\right)-Q_E=0 \tag{2}$$

where ϕ is the porosity of the porous media, ρ denotes molar density, x is composition in mole fraction, S is saturation, V is volumetric flow, J is molar diffusion flux, which is usually ignored for large scale applications, and Q is a source or sink term. In Eq. (2), U denotes internal energy, H is enthalpy, and G is heat conduction flux. The subscript i denotes a given component while the superscript k denotes a given phase. Summations are over all phases $k=1,\ldots,P$. C is the total number of components in the mixture. The subscript M in Eq. (2) denotes the rock media whereas the symbol ∇ denotes the gradient of a vector.

3.2. Phase equilibrium in general form

Phase equilibrium in a finite volume cell (or grid block) is described by the equality of partial fugacities for all components in all phases, clearly a topic on which publications in the chemical engineering literature abound. In particular,

$$f_i^1=f_i^2=\cdots=f_i^k,\quad i=1,\ldots,C;\quad k=1,\ldots,P \tag{3}$$

where f_i^k denotes the partial fugacity of component i in phase k and is given by

$$f_i^k = x_i^k \varphi_i^k p \tag{4}$$

where φ is the fugacity coefficient of component i in phase k and p is pressure.

Conservation of mass within any grid block is represented by a set of component mass-balance equations

$$\rho_T z_i - \sum \rho^k S^k x_i^k = 0, \quad i = 1, \ldots, C \tag{5}$$

where ρ_T and z_i are the total density and mole fraction of component i in the cell. Note that there is some overlap in symbols because standard notation in reservoir engineering and chemical engineering thermodynamics each use the same symbol to denote different quantities. We caution the reader to pay careful attention to context so the meaning of a symbol is clear.

Finally, in the natural formulation, Eqs. (1)–(3) are solved simultaneously and do not require a separate solution of flash problem. For the molar formulation, overall composition, temperature, and pressure of a given finite volume are specified, and, as a consequence, Eqs. (3)–(5), which constitute the classical isothermal, isobaric (Tp) flash problem, must be solved separately for the number and type of equilibrium phases and their corresponding compositions and densities.

3.3. Equation of state

The topic of equations of state (EOS) is intimately familiar to the PSE and thermodynamics communities of chemical engineering and, in general, EOS are required to model reservoir fluids. This is because some of the components (e.g., CH_4, N_2, CO_2) and/or mixtures of components can be supercritical at various conditions of temperature and pressure in a reservoir. Using an EOS, all phase properties (i.e., density, fugacity coefficients, fugacities, chemical potentials, enthalpies, etc.) can be readily computed. Furthermore, cubic equations are preferred over more complex equations like Statistical Associating Fluid Theory because they have a lower computational overhead and provide results that are within acceptable accuracy. As described later in this article, GFLASH allows the user to select from a number of more commonly used cubic EOS.

3.4. Other constitutive equations

Other constitutive equations are also needed to close the numerical model and allow proper integration of Eqs. (1) and (2). These constitutive equations include Darcy's Law, heat conduction, and when relevant, diffusion equations – again all topics familiar to the PSE community in traditional applications such as heat and mass transfer in catalyst pellets, non-equilibrium models in multistage distillation, as well as more recent applications in bio-medical modeling and simulation of the brain among others.

3.4.1. Darcy's law

Darcy's law describes the volumetric flow of each phase, V^k, through porous media as

$$V^k = -\left(\frac{\kappa \hat{R}_i^k \rho^k x_i^k}{\mu^k}\right) \nabla(p + \rho^k x_i^k g z) \tag{6}$$

where κ is an intrinsic rock or soil permeability, $\hat{R}$ is relative permeability, μ is viscosity, g is the acceleration due to gravity, and z is the coordinate in the direction of gravity.

3.4.2. Heat conduction equations

The heat conduction equation is

$$G^k = -K^k \nabla T \tag{7}$$

where K is the thermal conductivity and T is absolute temperature.

3.5. Equation coupling

The conservation of mass and energy, flow, and conduction through porous media described by Eqs. (1)–(7), and the equations describing the conservation of mass, conservation of energy with heat losses to the surroundings, and phase equilibrium form a large system of strongly coupled nonlinear algebraic equations. In a hierarchical sense, the EOS lies at the innermost level of the computations and provides the phase densities. Phase densities are used to calculate fugacity coefficients, and fugacities to determine the type and amounts of each phase present in a grid block (i.e., by solving the traditional chemical engineering Tp flash). GFLASH calculated phase densities and composition are then used to determine the unknown variables at the reservoir level (e.g., pressures, saturations, and temperatures) as well as heat conduction fluxes, and the flow of phases through the porous media.

4. Implementation

As noted in the literature survey, several computer implementations and methods of solving the model equations described in Section 3 are available. In this subsection, we describe the specific implementation of the reservoir model, well models, and constitutive equations associated with heat conduction. The reservoir modeling software is called Automatic Differentiation – General Purpose Research Simulator (AD-GPRS). AD-GPRS was originally developed and is currently maintained by the SUPRI-B group in the Energy Resources Engineering Department at Stanford University. It enjoys widespread use throughout the reservoir and petroleum engineering communities. AD-GPRS is written in C++. The EOS and flash calculations are implemented in a suite of FORTRAN programs called GFLASH, which was developed and is maintained by A. Lucia, and may be of particular relevance to the PSE community.

4.1. AD-GPRS

AD-GPRS is an advanced reservoir simulator with wide ranging capabilities that include

1) flexible treatment of all nonlinear physics,
2) a fully thermal-compositional formulation for any number of phases,
3) multi-phase CSAT for efficient and robust computation of phase behavior,
4) a variety of discretization schemes in time and space,
5) thermal geo-mechanical modeling including the effects of fractures,
6) a fully coupled, thermal, multi-segmented well model with drift-flux, and
7) an adjoint-based optimization module.

There are, of course, many details associated with AD-GPRS (Voskov & Zhou, 2012); its main features are summarized here.

4.1.1. Formulations

Both natural and molar formulations are available in AD-GPRS (Voskov & Tchelepi, 2012). Regardless of formulation, the primary

dynamic model equations describing the time evolution of material and energy in a reservoir given by Eqs. (1) and (2) are appended with a number of constraint equations to form a differential algebraic equation (DAE) system. The algebraic constraint equations include

1) fugacity constraints [i.e., Eq. (3)].
2) summation equations for the mole fractions in each phase.

$$1 - \sum_{i=1}^{C} x_i^k = 0, \tag{8}$$

3) saturation summation equations

$$1 - \sum_{k=1}^{P} S^k = 0, \tag{9}$$

4) volume balance constraints when total mass variables are used

$$\phi \rho_T \mathbb{V} - \sum_{i=1}^{C} n_i = 0, \tag{10}$$

where n_i is the overall number of moles of component i in a grid block (fixed for each GFLASH calculation) and $\mathbb{V}$ is the volume of a grid block.

Eqs. (1), (2), (3), (6), (7), (8), (9), and (10) comprise a DAE representation of the reservoir equations.

4.1.2. Discretization

The DAE system described by Eqs. (1), (2), (3), (6), (7), (8), (9), and (10), is converted into a set of nonlinear algebraic equations using finite volume spatial and temporal discretizations. Note that Eqs. (1), (2), (3), (6), (7), and (8) are essentially the same equations used to model traditional steady and unsteady-state chemical processes.

4.1.2.1. Spatial discretization. Spatial representation of a reservoir in discrete form in AD-GPRS uses the Multi-Point Flux Approximation to account for the geometry of fluxes across interfaces (see Zhou et al., 2011 for details). Consider the flux across the interface shared by two cells, denoted by j and j_1, and assume that the normal vector at the interface has an orientation that points into cell j. The overall flux of component i from j_1 to j is given by

$$F^{j,j_1} = \sum_{k=1}^{P} x_i^k \rho^k \lambda^k (\Phi^{j,j_1})^k \tag{11}$$

where λ^k is the mobility of phase k. Here all quantities except $(\Phi^{j,j_1})^k$ are taken in upstream of flow direction. $(\Phi^{j,j_1})^k$ is called the geometric part of the flux of phase k and is approximated by

$$(\Phi^{j,j_1})^k = \sum_{k=1}^{P} \theta^{j,j_1} \left[p_j^k - p_{j_1}^k + g(\gamma^{j,j_1})^k d^j \right] \tag{12}$$

where the summation in Eq. (12) is over the number of data points associated with the flux across interface $\{j, j_1\}$ (only one for a Two-Point Flux Approximation), $\theta^{j,j_1} > 0$ is the transmissibility coefficient average on interface $\{j, j_1\}$, d^j is the depth of cell j, and $(\gamma^{j,j1})^k$ is the mass density of phase k averaged at the interface $\{j, j_1\}$.

Similarly heat (energy) flux can be expressed as

$$E^{j,j_1} = \sum_{k=1}^{P} [\rho^k H^k \lambda^k (\Phi^{j,j_1})^k + S^k K^k \theta_g^{j,j_1} (T_j - T_{j_1})] \tag{13}$$

where θ_g^{j,j_1} is the geometrical part of the transmissibility coefficient assuming Two-Point Flux Approximation (TPFA) for the conduction term (Voskov and Zhou, 2012).

4.1.2.2. Temporal discretization. Temporal discretization by implicit integration is unconditionally stable. AD-GPRS has a number of the commonly used temporal discretizations – FIM, IMPES, IMPSAT, and AIM. As noted in Section 2, each of these methods represents a different approach where different unknown variables and equations are treated either explicitly or implicitly. In AD-GPRS, FIM, IMPES, and IMPSAT are all considered special cases of AIM. Finally, Courant–Friedrich–Lewy (CFL) stability criteria are used to adaptively determine the level of implicitness to solve the model equations.

4.1.3. Solution of nonlinear algebraic equations

After assembling the Jacobian matrix, the Newton–Raphson method solves the linear system of equations at each iteration. The relations, other than the mass conservation equations, are treated as constraints that are local to a grid block. To minimize the size of the global linear system, a Schur-complement procedure is applied to the full Jacobian matrix of each block to express the primary (mass conservation) equations as a function of the primary variables only (Cao, 2002). After the size of the system is reduced, the resulting global linear system of equations is solved for the primary variables. An iterative linear equation solver with pre-conditioning is used to solve the linear system.

After the linear system is solved, the computed changes to the primary variables are used with the secondary equations to determine changes in the secondary variables locally in each grid block. Next, the nonlinear variables are updated using different strategies and safeguards to ensure that the solution remains within physical boundaries. Convergence of Newton–Raphson iteration depends on aspects that include (1) any corrections to updated variables that employ safeguards, (2) various chopping strategies for different unknowns, and (3) the choice of time step. Several strategies for updating variables and time-step choice are implemented in AD-GPRS (Voskov and Zhou, 2012).

4.1.4. Phase behavior computations

In this section, different approaches to phase behavior computations in AD-GPRS are described including the use of intermittent flash solutions and CSAT.

4.1.4.1. Intermittent flash problem solutions. For phase behavior computations, AD-GPRS uses a two-stage procedure. In the first stage, the number of phases that exist in each grid block is determined. This can be obtained using Gibbs energy minimization or phase stability analysis (Michelsen, 1982a). In the second stage, flash calculations are performed to determine the compositions of the existing phases (Michelsen, 1982b). At both stages a combination of Successive Substitution Iteration and Newton's method is used.

As an alternative to this two-stage strategy, a generalization of the negative-flash based approach of Whitson and Michelsen (1989) can be used (Iranshahr et al., 2010). Here it is assumed that the number of phases present is the maximum possible, and then Eqs. (3) and (5) are solved, allowing for phase fraction to be less than zero, or greater than one. When the phase fractions of a converged negative flash procedure are negative, fewer existing phases are assumed and a similar procedure for this reduced system may be required (Iranshahr et al., 2010).

4.1.4.2. Compositional space adaptive tabulation (CSAT). Solving flash problems for all grid blocks over all nonlinear iterations and time steps is computational demanding. To improve the performance of phase behavior computations in reservoir simulation, the CSAT approach originally developed by Voskov and Tchelepi (2009a,b) is used. CSAT adaptively stores a discrete set of tie-lines at different pressures and temperatures to represent phase behavior

during reservoir simulation. This collection of tie-lines is interpolated and used to look up the phase state of the mixture at a particular pressure and temperature. In addition, the number of tie lines is collected adaptively based on the specific attributes of a compositional solution during a reservoir simulation.

CSAT completely replaces the need for phase stability tests and provides good initial guesses for the standard *Tp* flash computations.

4.1.4.3. Compositional space parameterization (CSP). The compositional space parameterization (CSP) method (Voskov & Tchelepi, 2009a; Zaydullin et al., 2013) is based on casting the nonlinear governing equations (1) and (2), including thermodynamic phase equilibrium constraints (3), in terms of the tie-simplex (γ) space. During a simulation, the γ space is adaptively discretized using supporting tie-lines. The coefficients for the governing system of equations, including the phase compositions, densities, and mobilities, are computed using multi-linear interpolation in the discretized space.

Using the CSP methodology, phase behavior computations can be replaced by an iteration-free look-up table procedure during the course of a reservoir simulation, removing the need for standard EOS computations (phase stability and flash). Also, it is important to note that the error associated with multi-linear interpolation is bounded and decreases with grid (or γ space) refinement (Zaydullin et al., 2013) and therefore only a limited number of supporting tie-lines are needed for the accurate representation of phase behavior. That, in turn, leads to significant gains in computational efficiency.

Tie-lines or tie-simplexes needed for CSAT and CSP can be parameterized using the generalized negative flash procedure (Iranshahr et al., 2010) or with GFLASH (Section 4.2).

4.2. GFLASH

GFLASH is a FORTRAN suite that models and solves the traditional chemical engineering multi-phase, multi-component isothermal, isobaric (*Tp*) flash problem. That is, given an overall composition for a fluid mixture, a temperature, and pressure, GFLASH determines the number of phases that exist at equilibrium and their corresponding compositions, fugacities, densities, and enthalpies. In this section, formulations, overall solution strategies, and methods of solution are described.

4.2.1. Equations of state

A number of the commonly used cubic EOS with and without volume translation are implemented in GFLASH. The EOS available include the

1) Soave–Redlich–Kwong (SRK) equation (Soave, 1972),
2) SRK with the Peneloux volume translation (SRK+) equation (Peneloux et al., 1982),
3) Predictive SRK (PSRK) equation (Holderbaum & Gmehling, 1991),
4) Electrolyte PSRK (ePSRK) equation (Kiepe et al., 2004),
5) Peng–Robinson (PR) equation (Peng & Robinson, 1976),
6) volume translated PR (VTPR) equation (Ahlers & Gmehling, 2001; Ahlers & Gmehling, 2002), and
7) multi-scale Gibbs–Helmholtz Constrained (GHC) equation (Lucia et al., 2012).

4.2.1.1. Formulation and solution. All EOS are formulated as cubic polynomials in compressibility factor, z, in the complex plane in the form

$$f(z) = c_1 z^3 + c_2 z^2 + c_3 z + c_4 = 0 \tag{14}$$

The resulting single variable function, $f(z)$, is solved using Newton's method in the complex plane to find any root to an accuracy of $|f(Z)| \le 10^{-12}$. The cubic polynomial is then deflated to a quadratic equation, which is solved using the quadratic formula to determine the other two roots. This approach removes the need to use an accurate initial guess for Newton's method, guarantees that all three roots will always be found, and is actually faster than using the analytical solution to a cubic polynomial.

4.2.1.2. Root assignment. Correctly determining which root is liquid and which root is vapor is as important, if not more important, than computing roots to EOS and is particularly challenging under harsh conditions (i.e., high T and high p). The current approach used to assign roots in GFLASH is as follows: For a set of roots given by $\{z_1, z_2, z_3\}$, where any root has the complex variable form $z_k = a_k \pm b_k$, $k = 1, 2, 3$, we define

$$Z^L = \min(|Z_i|) \quad \text{and} \quad Z^V = \max(|Z_i|) \tag{15}$$

where $|z_k|$ denotes the complex absolute value function given by $|Z_i| = \sqrt{a_i^2 + b_i^2}$ and the superscripts L and V denote liquid and vapor, respectively. Phase densities are easily computed from the compressibility factors, z^L and z^V, using the expression

$$\rho = \frac{p}{z^k RT} \tag{16}$$

4.2.2. Flash problem formulations and method of solution

The flash problem is really two problems – a phase stability problem and a phase equilibrium problem. In GFLASH, the formulations of the phase stability and phase equilibrium conditions use the dimensionless Gibbs free energy of mixing, $\Delta G/RT$, and the dimensionless Gibbs free energy, G/RT, respectively.

4.2.2.1. Phase stability. Minima in $\Delta G/RT$ often turn out to be inexpensive and good approximations for points of tangency. The necessary conditions for a minimum in $\Delta G/RT$ are formulated in terms of the equality of dimensionless chemical potentials, μ_i, $i = 1, \ldots, C$. For the phase split (or phase stability) problem, which is always a two-phase determination, the model equations are given by

$$F(x) = \frac{\left[(\mu_1 - \mu_i^0) - (\mu_C - \mu_C^0)\right]}{RT}, \quad i = 1, \ldots, C-1 \tag{17}$$

where the superscript 0 denotes standard state and the unknown variables in Eq. (17) are the mole fractions, x_i, $i = 1, ..., C-1$, of a single hypothetical phase. Note that this formulation of the phase split problem results from the projection of the dimensionless Gibbs free energy of mixing onto the summation equation [i.e., Eq. (8)].

4.2.2.2. Phase equilibrium. Phase equilibrium equations are also formulated in terms of dimensionless chemical potentials using projection onto the conservation of mass equations. Conservation of mass for the phase equilibrium problem is given by

$$n_i - \sum n_i^k = 0, i = 1, \ldots, C \tag{18}$$

where n_i is the overall moles of component i in the system and is fixed, n_i^k is the number of moles of ith component in the kth phase, and the summation in Eq. (18) is over all phases. Note that the phase equilibrium problem is formulated in terms of mole numbers, not mole fractions, because it is a way of exploiting many of the useful mathematical properties of partial molar quantities.

Phase equilibrium is defined by the equality of dimensionless chemical potentials given by

$$\frac{\mu_i^1}{RT} = \frac{\mu_i^2}{RT} = \cdots = \frac{\mu_i^k}{RT}, \quad i = 1, \ldots, C; \quad k = 1, \ldots, P \tag{19}$$

for any number of total phases, P. Eq. (19) is expressed in the form

$$F(n_i^1, n_i^2, \ldots, n_C^p) = \left(\frac{\mu_i^1}{RT} - \frac{\mu_i^k}{RT}\right) = 0, \quad i = 1, \ldots, C; \quad k = 1, \ldots, P \tag{20}$$

and then projected onto the mass balance constraints in Eq. (18) to reduce the size of the phase equilibrium problem and to ensure that conservation of mass is satisfied at each iteration.

4.2.2.3. Other modeling capabilities in GFLASH. GFLASH also has the capability of solving chemical reaction equilibrium problems and combined chemical and phase equilibrium problems, topics that are both familiar to the PSE community and important in various applications of EOR. For example, in applications of STRIP, partial oxidation of methane is used to generate in situ CO_2 and steam. In other EOR applications, where production water is re-used in order to defray the high cost of purchasing municipal water or expensive water treatment, salt precipitation in the presence of multiple fluid phases, which is a combined chemical and phase equilibrium problem, can be a serious operational problem. These sub-problems are also solved by Gibbs free energy minimization within the GFLASH framework.

4.2.2.4. Method of solution. GFLASH uses a trust region method to solve both the phase stability and phase equilibrium model equations. This methodology is a simple version of the terrain methodology developed by Lucia and Feng (2003). When applied to phase stability and phase equilibrium, we restrict the terrain method to look for only one stationary point in each of $\Delta G/RT$ and G/RT respectively.

In addition, when solving flash problems, GFLASH alternates between phase stability and phase equilibrium sub-problems, maintaining a monotonically decreasing sequence of values of G/RT until a global minimum identifying the number and type of phases as well as their associated mole numbers is found. Phase stability problems [i.e., Eq. (17)] are solved to an accuracy of $||F(x)||_2 \leq 10^{-6}$, where $||\cdot||_2$ denotes the 2-norm or Euclidean norm. In contrast, phase equilibrium problems (Eq. (20)) are solved to an accuracy of $||F(n)||_2 \leq 10^{-4}$ for two-phase equilibria and 10^{-5} for three-phase equilibria.

4.3. The connection between CSAT and GFLASH

In this section, we describe the connection between rigorous phase stability and flash computations using GFLASH and CSAT. We also describe the interface between AD-GPRS and GFLASH.

4.3.1. Conventional phase behavior computations

The number and types of phases (or phase state) of a mixture in a given grid block can vary. For example, for mixtures that exhibit three-phase behavior, there are seven different possible phase states – three single phase states (i.e., water-rich liquid, vapor, or oil-rich liquid), three different two-phase states (i.e., LLE, water-rich VLE, or oil-rich VLE), or vapor-liquid-liquid equilibrium (VLLE). Thus, the phase state as well as all corresponding phase compositions need to be determined for every grid block on each Newton iteration. For the natural formulation, a three-step procedure is usually used for these computations:

1. For any grid block, the current phase state is determined using a phase stability test.
2. If the current phase state is different from one on a previous Newton iteration, flash computations are performed to obtain phase compositions.
3. Phase properties (i.e., fugacities, densities, enthalpies, etc.) are obtained using known phase compositions.

Because of the complexity of the ADGPRS-GFLASH interface, both a phase stability test and flash computations are performed simultaneously.

4.3.2. Phase behavior computations with CSAT

As noted, CSAT can significantly improve the time required for phase behavior computations in fully compositional reservoir simulation (Voskov & Tchelepi, 2009a; Voskov & Tchelepi, 2009b). The general multiphase implementation of CSAT (Iranshahr et al., 2010; Voskov & Tchelepi, 2009b) is a two-step procedure:

1. Computation of supporting tie-simplexes (i.e., tie-triangles for three-phase systems).
2. Parameterization of tie-simplex subspace (tie-triangle planes for three-phase systems).

In the original CSAT implementation of Iranshahr et al. (2010), a generalization of the negative-flash idea (Whitson & Michelsen, 1989) for Step 1 and geometrical parameterization (i.e., tracking tie-lines from each side of a tie-triangle) for Step 2 was used. While this approach proves to be robust for challenging three-phase systems, it requires some preliminary knowledge of a multiphase mixture under investigation because the geometry of tie-simplex subspace can be quite complicated.

In this work, we have used a different strategy. First, we use GFLASH to provide fugacities for given pressure, temperature, and phase compositions and the generalized negative flash approach (Iranshahr et al., 2010) is used to find a supporting tie-simplex for the CSAT procedure. Next, an extension of the tie-simplex is adaptively discretized and GFLASH determines the phase state of a model cell. Finally, the collection of tie-simplexes and their extensions are interpolated for a particular pressure and temperature and used to look up the phase state of the mixture.

4.3.3. AD-GPRS/GFLASH interface

Because AD-GPRS is written in C++ and GFLASH is a FORTRAN suite, the proposed modeling and simulation framework is necessarily mixed language and therefore an interface is needed to communicate information between the two programs. The interface program is described in Appendix A.

5. Thermal EOR methodologies

In this section, steam injection and STRIP are introduced along with common performance metrics used to evaluate thermal EOR methods. We refer the reader to the work of Aziz et al. (1987), which is the 4th SPE Comparative Solution Project: Comparison of Steam Injection Simulators, for an introduction to steam injection and associated simulation challenges.

5.1. Steam injection

Steam injection is generally implemented using surface facilities to generate superheated steam, which is injected into a reservoir through a well. The entering steam heats the formation and lowers oil viscosity, which allows the oil to flow more easily to production wells. In all steam injection methods, surface generation of steam suffers from a number of disadvantages, not the least of which is energy losses (up to 50%) in the piping system and injection well.

5.2. Solvent thermal resource innovation process (STRIP)

STRIP, which has been developed by RII North America, is an environmentally friendly approach to EOR, which is deployed into existing wells, so there is little or no disruption of land. Unlike other steam injection processes, STRIP generates steam and CO_2 by in situ combustion of methane in oxygen, which eliminates energy losses to the injection well and delivers steam directly to the formation. STRIP also provides a co-solvent, CO_2, which enhances oil recovery by swelling oil and lowering viscosity. The STRIP burner can be placed in a number of configurations, but in this work the STRIP burner resides in a vertical section of the injection well. Because the combustion temperature can approach 3000 °C, the STRIP burner is typically cooled using production water, significantly reducing and often removing the need for municipal water. The nominal composition of lumped gases entering a reservoir formation is around 10 mol%, with roughly 6.7 mol% being CO_2.

5.3. Performance metrics

Several common metrics are used to evaluate the performance of a thermal EOR methodology. These metrics include (1) sweep and (2) oil recovery, which, of course, is of primary interest.

6. Numerical examples

In this section, two reservoir simulation examples are presented to elucidate key points, to compare the performance of steam injection and STRIP, and to demonstrate the reliability and computational efficiency of the numerical tools in GFLASH and AD-GPRS. However, prior to presenting results for reservoir simulation with STRIP, a number of traditional chemical engineering sub-problems needed to be solved, including a chemical equilibrium problem, an adiabatic flame temperature problem, and a salt precipitation problem, to clarify and quantify various aspects of the reservoir simulations. All reservoir simulation runs were performed using an Intel(R) Core(TM) 2 Duo CPU E6750 @2.66 GHz, 1.95 GB of RAM.

6.1. Example 1: chemical equilibrium of STRIP combustion

As noted, STRIP generates in situ CO_2 and steam by partial oxidation of methane. In a typical application, the reactants are fuel-rich and thus there are a number of 'major' syngas by-products such as H_2 and CO, and un-reacted methane and O_2 in addition to the CO_2 and steam. However, the composition of the combustion product stream is a function of both the O_2/CH_4 ratio and the reaction temperature, the latter of which we do not know. The O_2/CH_4 ratio, which is denoted by r, is an operational decision based on extensive laboratory experimentation and can vary between at 1.6 and 1.9 depending on the application. Note that the stoichiometric ratio of oxygen/methane for complete combustion is 2 and thus STRIP combustion is fuel-rich and thus will produce some syngas (H_2 and CO).

The governing equations for this single vapor phase chemical equilibrium problem are

$$\min \frac{G}{RT} = \sum_{i=1}^{C} \frac{n_i \mu_i}{RT} \tag{21}$$

subject to mass balances for hydrogen, oxygen, and carbon

$$\sum_{i=1}^{n} a_{ij} n_i = A_j, \quad j = 1, \ldots, J \tag{22}$$

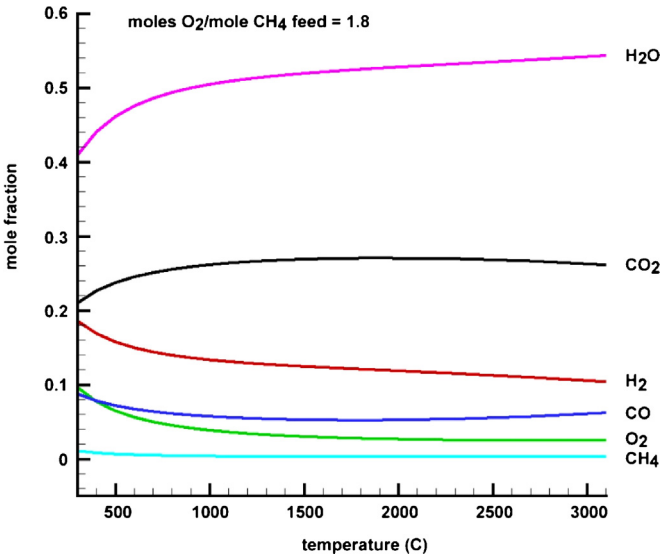

Fig. 1. STRIP combustion product composition vs. temperature for an fuel-rich burner.

where J is the number of atomic species, A_j is the total amount of atom j in the system, and a_{ij} is the number of jth atoms in the ith molecular compound. For this example using a basis of 1 mole of CH_4, the mass balances are

$$\text{hydrogen}: \quad 2n_{H_2} + 0n_{O_2} + 0n_{CO} + 4n_{CH_4} + 0n_{CO_2} + 2n_{H_2O} = 4 \tag{23}$$

$$\text{oxygen}: \quad 0n_{H_2} + 2n_{O_2} + 1n_{CO} + 0n_{CH_4} + 2n_{CO_2} + 1n_{H_2O} = 2r \tag{24}$$

$$\text{carbon}: \quad 0n_{H_2} + 0n_{O_2} + 1n_{CO} + 1n_{CH_4} + 1n_{CO_2} + 0n_{H_2O} = r \tag{25}$$

Fig. 1 shows the effect of reaction temperature on the composition of STRIP combustion products for temperatures between 300 and 3100 °C at 20 bar. Note that above about 1000 °C, there is very little change in the composition of the combustion products.

Table 1 gives the details of a single chemical equilibrium computation for 2500 °C at 20 bar for an oxygen-to-methane ratio of 1.8. Note that there is a significant amount of 'major' by-product gases, about 20 mol%, and a net production of 0.269696 moles.

Table 1
Numerical results for chemical equilibrium of STRIP combustion.

Chemical species	Feed mole fractions	Product gas mole fractions
H_2	0	0.133035
O_2	0.6428571	0.028308
CO	0	0.042660
CH_4	0.3571428	0.002809
CO_2	0	0.280303
H_2O	0	0.512884
Total moles	2.8	3.069696

Table 2
Composition of production water and combined feed for STRIP.

Chemical species	Production water molality (mol/kg H_2O)	Mole fractions of combined feed
H_2	0	0.016793
O_2	0	0.003229
CO	0	0.006459
CH_4	0	0.000388
CO_2	0	0.043532
Na^+	1.100299	0.017692
K^+	0.007587	0.000122
Ca^{2+}	0.029479	0.000474
Cl^-	1.166844	0.018762
SO_4^{2-}	0.000023	3.68×10^{-7}
H_2O	0.983278	0.892549
Total		1.000000

6.2. Example 2: adiabatic flame temperature

While Fig. 1 gives chemical equilibrium results for a wide range of combustion temperatures, the actual temperature of the combustion products for a given set of conditions should be estimated using an adiabatic flame temperature calculation and is coupled to the previous chemical equilibrium problem because the temperature and composition are interdependent. However, because product gas compositions are relatively weak functions of temperature above about 1000 °C, we can effectively decouple the problems and solve the adiabatic flame temperature problem using the product gas compositions shown in Table 1. The corresponding problem formulation, which is rather simple and can be found in several undergraduate level thermodynamics textbooks, is shown in Eq. (26).

$$0 = \Delta H_R^0 + \sum_{i=1}^{C} \int_{T_0}^{T} n_i C_{p,i}\, dT \tag{26}$$

where ΔH_R^0 is the standard heat of reaction, T_0 is a reference temperature and equal to 25 °C, and $C_{p,i}$ is the heat capacity for the ith component. Data for ΔH_R^0 and $C_{p,i}$ are given in Appendix B. The calculated adiabatic flame temperature for an oxygen-to-methane ratio of 1.6 is 3343.975 °C.

6.3. Example 3: salt precipitation

Use of production water in EOR processes can reduce the cost of purchasing municipal water or operating an on-site water treatment plant and concomitantly lower environmental impact. The main challenge associated with the use of production water is the presence of ions and the potential for salt precipitation. To lower the potential for precipitation, production water can be mixed with clean water. In the case of STRIP, production water is mixed with in situ generated steam for two purposes – to generate additional steam and to cool the STRIP combustion burner. Table 2 gives an illustration of the compositions of production water and the combined feed for a STRIP application to a real reservoir in Saskatchewan, Canada before and after mixing. Note that production water analyses are generally reported as molality, whereas mass or mole fractions are generally used in flash calculations.

Table 3
Meta-stable flash solution to combined chemical and phase equilibrium problem.

Quantity	Mole fractions of combined feed	Aqueous liquid	Vapor
H_2	0.016793	7.9788×10^{-7}	0.033336
O_2	0.003229	2.8861×10^{-6}	0.006408
CO	0.006459	7.7968×10^{-7}	0.012821
CH_4	0.000388	1.7858×10^{-7}	0.000770
CO_2	0.043532	9.0811×10^{-5}	0.086332
Na^+	0.017692	0.033586	0
K^+	0.000122	0.000247	0
Ca^{2+}	0.000474	0.000961	0
Cl^-	0.018762	0.038027	0
SO_4^{2-}	3.68×10^{-7}	7.4585×10^{-7}	0
NaCl	0	0	0
H_2O	0.892549	0.924811	0.860333
Phase fraction	1.000000	0.496276	0.503724
Density (kg/m^3)		831.985	8.464
G/RT	2.53535	2.496677	

Table 4
Equilibrium and ion solubility products for Example 3.

Molecular salt	K_{sp}	Q_{sp}
NaCl	4.3516	4.9124
KCl	7.0513	0.033875
$CaCl_2$	1.9765	0.30040
Na_2SO_4	2.6759	0.000207
K_2SO_4	7.0259	9.8612×10^{-9}
$CaSO_4$	0.27929	2.5815×10^{-6}

The real concern regarding precipitation comes from the fact that the combustion products from STRIP are very hot and thus the amount of liquid available to dissolve ions, even after mixing, might be quite small if too much vaporization occurs. Remember, the main purpose of STRIP is to inject enough steam and CO_2 into the reservoir for improved oil recovery. What this means is that the desired fluid stream entering the reservoir (i.e., at the injection well bore) should have a relatively high vapor fraction, say between 0.7 and 0.8. To determine whether or not salt precipitation will occur, we must therefore solve a combined chemical and phase equilibrium flash problem at high temperature. Salt precipitation is a heterogeneous chemical equilibrium problem and must be determined by comparing equilibrium solubility products, K_{sp}, to ion solubility products, Q_{sp}, for all possible molecular salts as shown in Eq. (27).

$$\left.\begin{array}{l} K_{sp}^k > Q_{sp}^k, \text{ then aqueous liquid is under-saturated with molecular salt k} \\ K_{sp}^k = Q_{sp}^k, \text{ then aqueous liquid is saturated with molecular salt k} \\ K_{sp}^k < Q_{sp}^k, \text{ then the aqueous liquid is super-saturated with salt k} \end{array}\right\} \quad k = 1, \ldots, n_s \tag{27}$$

where n_s is the number of molecular salts. In this example, there are six possible molecular salts: NaCl, KCl, $CaCl_2$, Na_2SO_4, K_2SO_4 and $CaSO_4$. The standard Gibbs free energy and enthalpy of formation data used to compute K_{sp} is shown in Appendix B. Moreover, it is entirely possible to compute multi-phase equilibrium flash solutions that are supersaturated and meta-stable; thus simultaneously satisfying conditions of multi-phase and chemical equilibrium is quite challenging. Table 3 shows a meta-stable VLE flash solution for the combined feed in Table 2 at 255 °C and 18 bar computed using the GHC equation of state.

Note that the supersaturated VLE solution has a lower value of G/RT than the single phase solution. Table 4 gives the values of K_{sp} and Q_{sp} for all six molecular salts at aqueous liquid phase conditions given in Table 3. Note that Table 4 clearly shows that $K_{sp}^{NaCl} < Q_{sp}^{NaCl}$

Table 5
Global minimum solution to combined chemical and phase equilibrium problem.

Quantity	Mole fractions of combined feed	Aqueous liquid	Vapor	Solid salt
H_2	0.016793	6.8490×10^{-7}	0.023735	0
O_2	0.003229	2.3922×10^{-6}	0.004563	0
CO	0.006459	6.4952×10^{-7}	0.009129	0
CH_4	0.000388	1.4567×10^{-7}	0.000548	0
CO_2	0.043532	7.1298×10^{-5}	0.061500	0
Na^+	0.017692	0.033746	0	0
K^+	0.000122	0.000419	0	0
Ca^{2+}	0.000474	0.001629	0	0
Cl^-	0.018762	0.037426	0	0
SO_4^{2-}	3.68×10^{-7}	1.2654×10^{-6}	0	0
NaCl	0	0	0	1.000000
H_2O	0.892549	0.926701	0.900524	0
Phase fraction	1.000000	0.290190	0.701886	0.007924
Density (kg/m^3)		813.901	8.245	2166.642
G/RT	2.53535	1.80108		

and therefore NaCl will precipitate. The molar amount that will precipitate, S_{NaCl}, is easily computed using the following mass balance

$$S_{NaCl} = Fx_{NaCl} - [c]_{Na^+}(n_{H_2O}MW_{H_2O})/1000 \quad (28)$$

where Fx_{NaCl} is the molar amount of NaCl in the feed, $[c]_{Na^+}$ is the solubility limit of Na^+ in the aqueous liquid, n_{H_2O} is the number of moles of water in the aqueous liquid, and MW_{H_2O} is the molecular weight of water.

Table 5 gives the global minimum vapor-liquid-solid equilibrium solution for the same combined feed conditions and there are several important points to note regarding this equilibrium solution.

1. The VLE + salt solution has a lower dimensionless Gibbs free energy than either the single phase solution or the supersaturated VLE solution.
2. The STRIP criterion of 0.7–0.8 vapor fraction has been met in the final solution.
3. Salt precipitation is potentially a serious concern in this application of STRIP unless production water is mixed with clean water.

6.4. Example 4: flash level reliability testing

A high level of reliability is needed at the flash level for successful reservoir simulations. Even a single failure in one grid block can cause the entire reservoir simulation to fail. To ensure reliability at the flash level, several phase diagrams similar to the ones shown in Fig. 2 and covering the entire composition space are usually generated using GFLASH for a number of different temperatures and pressures prior to running a reservoir simulation. Typically a composition interval of 0.005 is used for each independent composition. Thus, for a three-component mixture, roughly 20,000 composition points are generated for each temperature and pressure.

This is to ensure that phase boundaries are smooth and that changes in V-only, L-only, VLE, LLE, and VLLE regions make physical sense. Table 6 gives computational details for the rigorous flash tests.

Table 6
Statistics for rigorous flash solutions for CO_2–decane–water at 30 bars using GFLASH.

	$T = 373$ K	$T = 473$ K
No. of problems	19,532	19,532
No. of liquid-only solutions	687	1559
No. of vapor-only solutions	5	1775
No. of VLE solutions	1876	11,720
No. of LLE solutions	3207	682
No. of VLLE solutions	13,757	3796
No. of function calls	2,114,553	3,255,481
No. of EOS solves	5,448,233	7,709,004
Total solve time (CPU sec)	38.7	26.5

6.5. Example 5: comparison of steam injection and STRIP

This first EOR example compares model results for steam injection and STRIP for a 3D heterogeneous reservoir formation

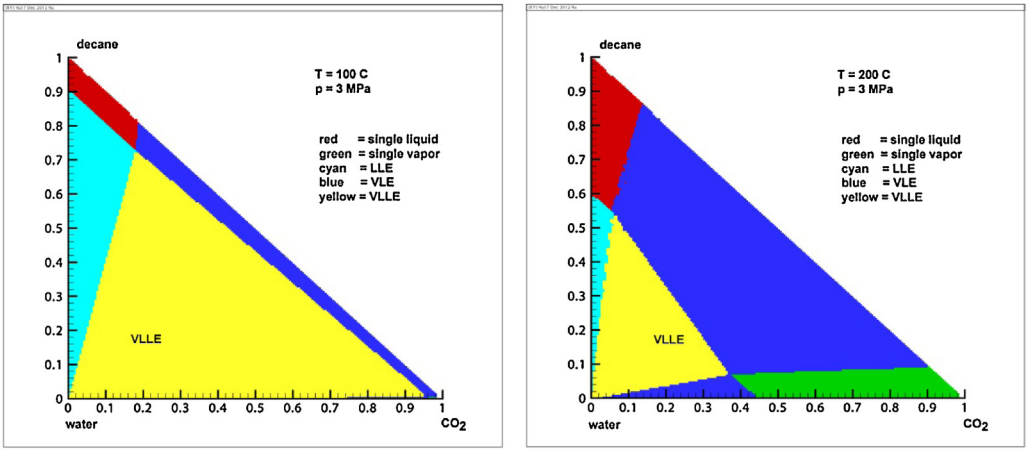

Fig. 2. CO_2–decane–water phase behavior at 100 °C and 200 °C and 30 bars.

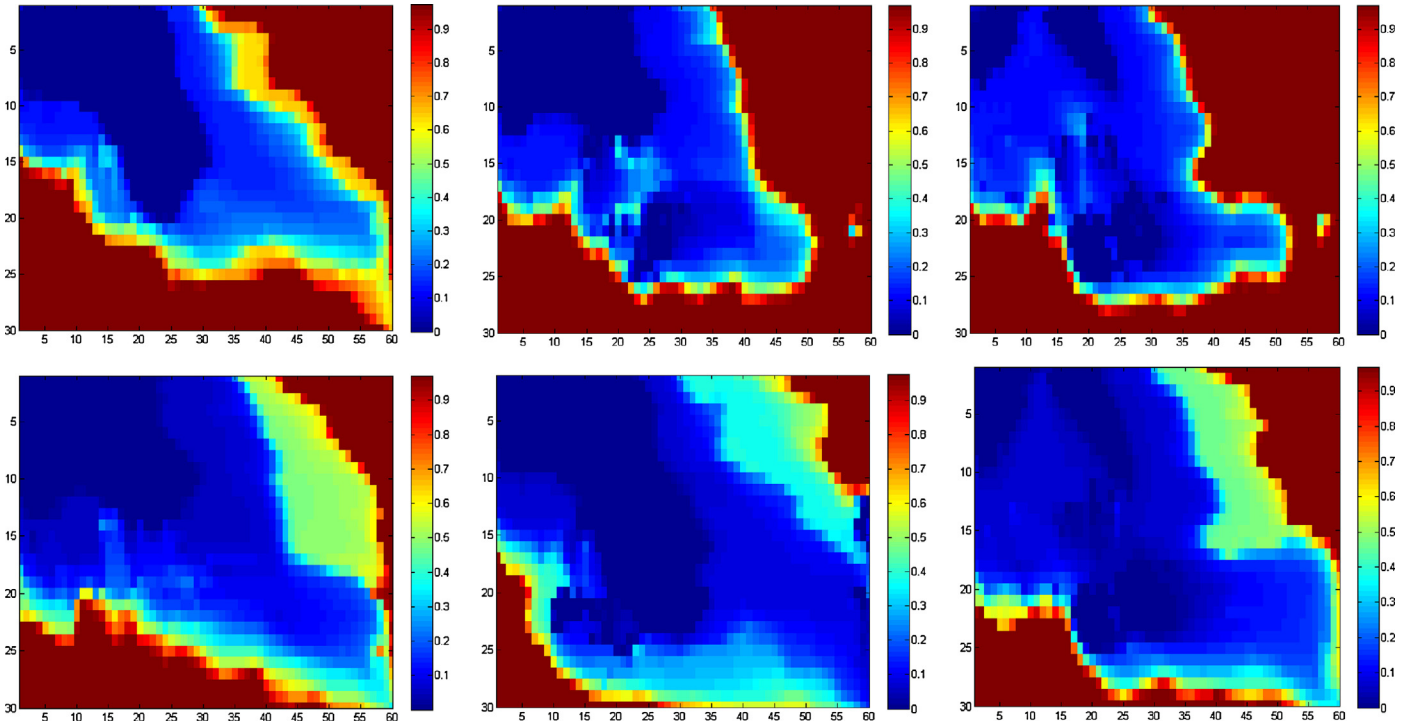

Fig. 3. Oil Saturation for Steam Injection (left) and STRIP (right) for Example 5.

Table 7
Input data for Example 5.

Quantity	Value
Reservoir dimensions	$360 \times 360 \times 3.6\,m^3$
Initial reservoir T and p	290 K, 31 bar
Initial reservoir composition	1 mol% CO_2, 74 mol% oil, 25 mol% water
Porosity, rock heat capacity	0.197% (average), 2.35×10^6 J/m^3 K
Permeability (Upscaled SPE10)[a]	5 orders of magnitude in permeability variations
Injection conditions	Water rate 15 m^3/day heat rate 1.3×10^{10} J/day (steam at 518 K)
Injection composition	10% CO_2, 90% water (STRIP) 1% CO_2, 99% water (steam injection)
Production well p	3.45 bar
Time horizon	2000 days

[a] Taken from Christie and Blunt (2001).

containing light oil. Input data are listed in Table 7. In EOR applications it is typical to 'lump' components to reduce computational costs; thus for STRIP all light gases were treated as CO_2, which is the solvent of interest.

In this example, the model is based on a fragment of the upscaled SPE10 porosity and permeability fields (see Christie & Blunt, 2001). Here we used a grid size of $30 \times 60 \times 3$ m^3 with uniform gridblock volume of $12 \times 6 \times 1.2$ m^3. The injection and production wells were placed at opposite corners of the reservoir. A single component, n-decane, was used to model the oil and the EOS used was the SRK equation. Steam injection was modeled using an injection stream of 1 mol% CO_2 and 99 mol% steam while STRIP, which contains more CO_2 from combustion, injected 10 mol% CO_2 and 90 mol% water. The heat and water input were the same for steam injection and STRIP so an equitable comparison could be drawn.

6.5.1. Main simulation results

The performance of steam injection and STRIP are compared using the metrics of sweep efficiency and oil recovery.

6.5.1.1. Sweep efficiency. The sweep efficiency can be deduced from oil saturation at the end of the operating period.

Fig. 3 shows the oil saturation in the reservoir for steam injection and STRIP after 2000 days of operation.

Note that the blue regions are much larger for STRIP than for steam injection, indicating that STRIP removes more oil. One can also make more quantitative measures of sweep efficiency using the following expression

$$\eta = \frac{V_{oil}^{\Delta}}{V} \tag{29}$$

where η denotes the sweep ratio, V_{oil}^{Δ} is the porous volume for which the oil composition has changed by 1% or more and V is the total porous volume available to the oil. Fig. 4 shows quantitative results for sweep ratio for steam injection and STRIP as a function of time. The sweep ratios for steam injection and STRIP after 2000 days of operation are 60% and 83%, respectively. Clearly the sweep ratio of STRIP is superior to steam injection.

6.5.1.2. Oil production. Fig. 5 shows the total cumulative oil recovered during 2000 days of operation of steam injection and STRIP.

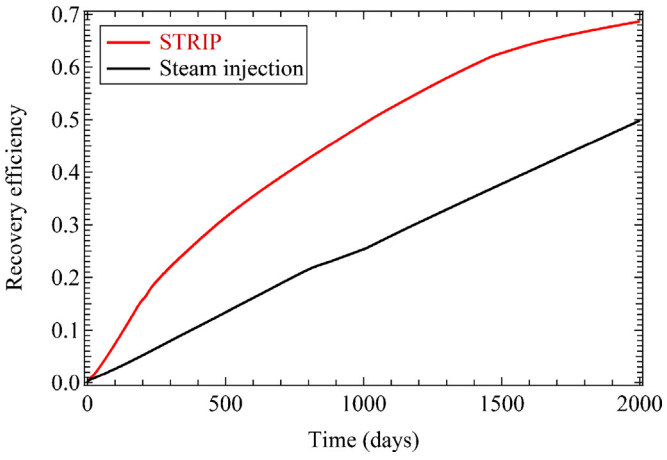

Fig. 4. Sweep ratio for steam injection and STRIP for Example 5.

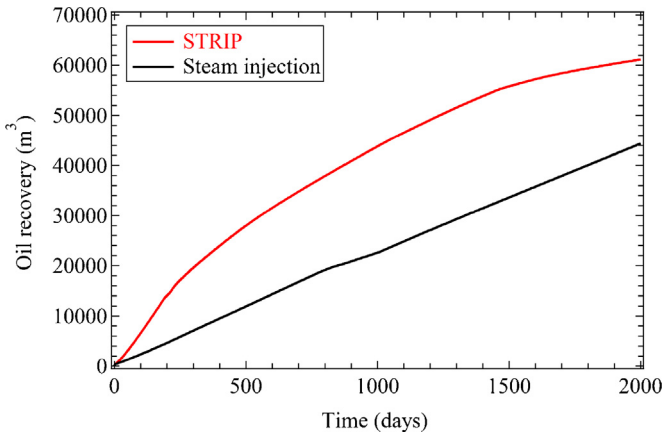

Fig. 5. Oil Recovery for Steam Injection and STRIP for Example 5.

To compare oil recovery, the Original Oil in Place (OOIP) at surface conditions, which is a common assumption in the petroleum industry, must be computed. OOIP is calculated using formula

$$\text{OOIP} = \sum_{\text{all blocks}} \frac{V\phi S_{oil}}{B_{oil}} \tag{30}$$

where V is the block volume, S_{oil} is oil saturation, and B_{oil} is the surface-to-reservoir formation volume factor. Here again, STRIP outperforms steam injection – recovering 16,764 m^3 (105,442 barrels) more oil and leaving less OIP after 2000 days. Table 8 summarizes the performance of steam injection and STRIP for this first example.

6.6. Example 6: comparisons between conventional EOS and CSAT

This second example compares a conventional reservoir simulation approach, which uses an EOS, to one that uses CSAT. For this example, pore volumes and permeability fields were taken from the upper layer of the original SPE10 model (Christie & Blunt, 2001). The simulations were performed using an initial reservoir composition of 1 mol% CO_2, 49 mol% *n*-decane, 20 mol% *n*-hexadecane, and 30 mol% water and the initial reservoir pressure and temperature were 31 bar and 300 K, respectively. One injection and one production well were placed at opposite corners of the reservoir. The injection well operates under constant pressure and temperature conditions of 60 bar and 500 K. The STRIP injection fluid consisted of 15 mol% CO_2, and 85 mol% water. The production well was set to a constant pressure of 3.45 bar. Input data for this example are shown in Table 9.

Table 8
Summary of steam injection and STRIP performance for Example 5.

	Steam injection	STRIP	Improvement with STRIP
Operation (days)*	2000	2000	
OOIP (m^3)	89,051	89,051	
Oil produced (m^3)	44,380	61,144	16,764
% oil recovered	50%	69%	38%
Sweep efficiency	60%	83%	27.4%

Table 9
Input data for STRIP simulation of Example 6.

Quantity	Value
Reservoir dimensions	$365 \times 670 \times 0.6096\ m^3$
Initial reservoir T & p	300 K, 31 bar
Initial reservoir composition	1 mol% CO_2, 49 mol% C_{10}, 20 mol% C_{16}, 30 mol% water
Average porosity	0.1945
Permeability (SPE10, upper layer)[a]	8 orders of permeability variations
Injection T & p	500 K, 60 bar
Injection composition	15% CO_2, 85% water
Production well p	3.45 bar
Time horizon	7000 days

[a] Taken from Christie and Blunt (2001).

6.6.1. Main simulation results

The details of the performance of STRIP are discussed along with the features of the simulator.

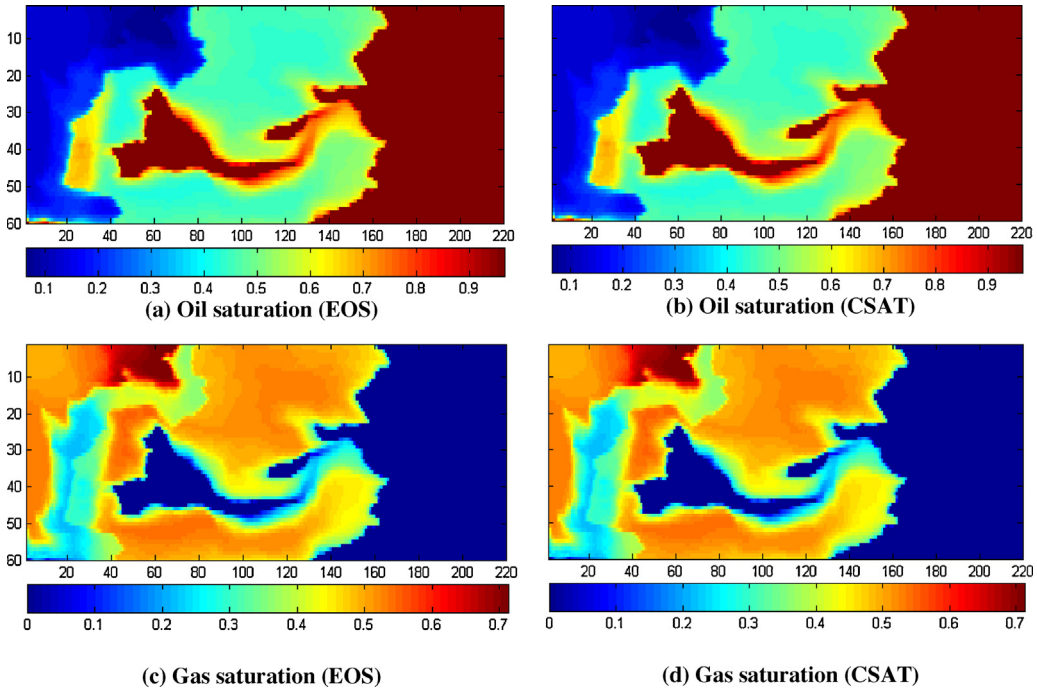

Fig. 6. Oil and gas saturation distributions for EOS and CSAT simulations after 7000 days.

Table 10
Statistics for STRIP reservoir simulation of Example 6.

	AD-GPRS/GFLASH	AD-GPRS/GFLASH/CSAT
Time horizon (days)	7000	7000
Average time step (days)	4.9	4.9
Model formulation	Natural Variables	Natural Variables
No. of grid blocks	13,200	13,200
No. of equations/grid block	2 + P-1 + (C-1)P	2 + P-1 + (C-1)P
Equation solving methodology	Fully Implicit Method (FIM)	Fully Implicit Method (FIM)
Total No. of Newton iterations	4140	4140
Total No. of EOS solves	44,028,736	499,693
Total flash solution time (CPU sec)	270,830	3869
Total simulation time (CPU sec)	345,659	79,710

6.6.1.1. Sweep efficiency. Oil and gas saturations provide enough information to quantify sweep efficiency. Fig. 6 shows the oil and gas saturation in the reservoir for STRIP after 7000 days of operation, where the *x* and *y* axes denote grid blocks and the color bar shows saturations.

As expected, both CSAT and GFLASH provide identical results for gas and oil saturation. This is because CSAT only skips phase identification and rigorous flash computations when compositions are far from phase boundaries.

6.6.1.2. Simulation statistics. Table 10 summarizes the simulation statistics for this example and shows that rigorous flash solutions take the bulk of the computer time for the conventional EOS approach. CSAT, on the other hand, significantly decreases the number of EOS solves and, therefore, reduces total flash solution time by almost two orders of magnitude.

7. Conclusions

A new methodology for reservoir simulation was presented. This new modeling and simulation framework consists of AD-GPRS, the Automatic Differentiation – General Purpose Research Simulator, a general multi-phase equilibrium flash suite, GFLASH, and a Compositional Space Adaptive Tabulation (CSAT) approach. The fundamental PDE model equations and methods of solution for the resulting nonlinear algebraic equations at the reservoir scale were provided. Modeling, equation-solving, and numerical details for four separate chemical engineering problems at the flash level of the computations were also presented to raise awareness in the PSE community with regard to reservoir simulation. Coupling of the flash and reservoir equations was described. CSAT and the interface between AD-GPRS, which is written in C++, and GFLASH, which is a FORTRAN program suite, were also described. Two numerical reservoir simulation examples were presented to highlight the accuracy, reliability, and computational efficiency of AD-GPRS/GFLASH, including two three-phase reservoir simulation examples with and without the use of CSAT for a highly heterogeneous reservoir formation and for three- and four-component system. Comparisons of steam injection and STRIP in Example 5 clearly demonstrate the superiority of the Solvent Thermal Resource Innovation Process in terms of sweep and oil recovery. Example 6 demonstrates that the AD-GPRS/GFLASH/CSAT framework reduces the simulation time by two orders of magnitude without losses in accuracy or reliability.

8. Coda

In addition to the chemical engineering sub-problems described in this work, there are also others, including sub-problems that require

(1) The characterization of oils with many components.
(2) Development of better methods for determining viscosity and relative permeability in harsh conditions.
(3) Understanding chemical EOR methods and the associated phase equilibrium in the presence of surfactants and other chemical additives.
(4) The determination of asphaltene precipitation.
(5) Reaction kinetics models for gas hydrate formation and CO_2 sequestration.
(6) Improved numerical methods for flash and for solving 'stiff' DAE systems.

In our opinion, the PSE community is ideally positioned to make contributions in these and other areas as they relate to reservoir simulation.

Appendix A. C++ interface for AD-GPRS/GFLASH

The C++ interface for communicating information between AD-GPRS and GFLASH is divided into two sections: a definition section and an execution section.

The definition section, which defines essential variable information, is shown below and is self-explanatory.

Table B.1
Standard heat of formation and ideal gas heat capacity data.

Species	ΔH_f^0 (kJ/mol)	A	B	C	D
H_2	0	27.14	9.274×10^{-3}	-1.381×10^{-5}	7.645×10^{-9}
O_2	0	28.11	-3.680×10^{-6}	1.746×10^{-5}	-1.065×10^{-8}
CO	−110.5	30.87	-1.285×10^{-2}	2.789×10^{-5}	-1.272×10^{-8}
CH_4	−74.5	19.25	5.213×10^{-2}	1.197×10^{-5}	-1.132×10^{-8}
CO_2	−393.5	19.80	7.344×10^{-2}	-5.602×10^{-5}	1.715×10^{-8}
H_2O(g)	−241.8	32.24	1.924×10^{-3}	1.055×10^{-5}	-3.596×10^{-9}

Interface: Definition Section

```
extern "C"
{
void GFLASH(  int *ncomps,            //number of components
          int *nsalts,                //number of salts or ions
          double *xsalts,             //salt compositions
          double *temp,               //temperature in K
          double *pres,               //pressure in bar
          double *feed,               //feed composition
          int *np_gprs,               //number of equilibrium phases
          double *gprs_xcp,           //equilibrium phase compositions
          double *gprs_nu,            //phase fractions
          double *gprs_fug,           //partial fugacities
          double *gprs_der_fug,       //partial fugacity derivatives
          double *gprs_rho,           //density
          double *gprs_der_rho,       //derivatives of density
          double *gprs_enth,          //enthalpy
          double *gprs_der_enth,      //derivatives of enthalpy
          int *ipflash,               //print flag
          int *mode,                  //flag to increase efficiency

          int *re_enter);             //cold start or start from previous solution
}
```

During execution, AD-GPRS passes GFLASH the number of components (ncomps), the temperature (temp), pressure (pres), and the feed composition (feed) for a given grid block. GFLASH returns the number of equilibrium phases (np_gprs), the phase compositions (gprs_xcp), the equilibrium phase partial fugacities (gprs_fug), their pressure, temperature and composition derivatives (gprs_der_fug), equilibrium phase densities (gprs_rho), densities derivatives (gprs_der_rho), equilibrium phase enthalpies (gprs_enth), and associated phase enthalpy derivatives (gprs_der_enth).

One variable that need some clarification is the integer variable RE_ENTER, which provides re-entry facilities in GFLASH, is defined as follows:

$$\text{RE\_ENTER} = \begin{cases} 0, & \text{GFLASH reads all input data for flash and solves the given flash problem.} \\ 1, & \text{skips reading input data but solves the given flash problem.} \\ 99, & \text{given np\_gprs, temp, pres, and gprs\_xcp, GFLASH does not solve a flash but calculates all phase fugacities, densities, enthalpies and their pressure, temperature and composition derivatives.} \end{cases}$$

RE_ENTER gives AD-GPRS complete control of GFLASH and is an important feature for reducing computational workload. RE_ENTER allows AD-GPRS to determine when it is necessary to solve a rigorous flash problem for a given grid block or when to skip solving the flash for that grid block. More specifically, when the rigorous solution of a flash problem is needed, AD-GPRS sets RE_ENTER = 0 or 1 and GFLASH solves a rigorous flash problem. As a result, the fugacity constraints for the given grid block are satisfied for the conditions of temperature, pressure and equilibrium phase compositions for the grid block and communicated back to AD-GPRS. On the other hand, when the temperature, pressure and equilibrium phase compositions for that grid block change but it is anticipated that the number of equilibrium phases in that grid block is unlikely to change, then AD-GPRS ask GFLASH to simply evaluate fugacities, densities, enthalpies, and their derivatives without solving a flash problem by setting RE_ENTER = 99. This approach works because AD-GPRS includes fugacity and other constraints in the equation set for a given time step, it converges the fugacity conditions defining equilibrium along with the conservation of mass and energy equations – whether or not they are satisfied at the beginning of the time step.

```
int main()
{
  int NC = 2;
  int NP = 2;
    // primary input
  double temp = 350.0;
  double pres = 34.0;
  vector<double> feed(NC, 0);
    // additional input
  int ipflash     = 0;
  int ncomps      = NC;
  int nsalts      = 0;
  int np          = NP;
  int mode        = 0;
  int re_enter    = 0;
    // output
  vector<double> xsalts(NC, 0);
  vector<double> xcp(NC*NP, 0);
  vector<double> nu(NP, 0);
  vector<double> fug(NC*NP, 0);
  vector<double> fug_deriv(NP*NC*(NC+2), 0);
  vector<double> gprs_rho(NP, 0);
  vector<double> gprs_der_rho(NP*(NC+2),0);
  vector<double> gprs_enth(NP, 0);
  vector<double> gprs_der_enth(NP*(NC+2),0);


GFLASH( &ncomps, &nsalts, &xsalts[0], &temp, &pres,
     &feed[0], &np, &xcp[0], &nu[0], &fug[0],
     &fug_deriv[0],&gprs_rho[0],&gprs_der_rho[0],
     &gprs_enth[0], &gprs_der_enth[0], &ipflash, &mode, &re_enter);

}
```

Table B.2
Standard Gibbs free energy and heat of formation data.

Species	ΔG_f^0 (kJ/mol)	ΔH_f^0 (kJ/mol)
Na^+	−261.88	−239.66
K^+	−282.28	−251.21
Ca^{2+}	−553.04	−542.96
Cl^-	−131.17	−167.46
SO_4^{2-}	−741.99	−907.51
NaCl	−384.1	−411.2
KCl	−408.3	−435.8
$CaCl_2$	−748.1	−795.8
Na_2SO_4	−1265.2	−1382.8
K_2SO_4	−1316.4	−1433.7
$CaSO_4$	−1320.3	−1432.7

Appendix B. Standard Gibbs free energy, standard heat of formation, and ideal gas heat capacity data

The standard heat of reaction, ΔH_R^0, is calculated using standard heats of formation data, $\Delta H_{f,i}^0$, plus the simple equation

$$\Delta H_R^0 = \sum_{i=1}^{prod} n_i \Delta H_{f,i}^0 - \sum_{i=1}^{react} n_i \Delta H_{f,i}^0 \quad \text{(B.1)}$$

Pure component ideal gas heat capacities are computed using a polynomial in temperature of the form

$$C_{p,i} = A_i T + B_i T^2 + C_i T^3 + D_i T^4 \quad \text{(B.2)}$$

Table B.1 gives the heat of formation data, which were taken from Appendix IV in Sandler (1999), and ideal gas heat capacity coefficient data, which have units of J/mol, taken from Reid et al. (1987).Table B.2 shows the standard Gibbs free energy and heat of formation data needed for computing equilibrium solubility products of molecular salts. Some of the data were taken from Sandler (1999) while the remaining data were taken from the CRC Handbook of Chemistry and Physics.

References

Acs, G. (1985). General purpose compositional model. *Journal of Petroleum Science and Engineering*, *25*, 543.

Ahlers, J., & Gmehling, J. (2001). Development of a universal group contribution equation of state. 1. Prediction of liquid densities for pure compounds with a volume translated Peng-Robinson equation of state. *Fluid Phase Equilibria*, *191*, 177.

Ahlers, J., & Gmehling, J. (2002). Development of a universal group contribution equation of state. 2. Prediction of vapor-liquid equilibria for asymmetric systems. *Industrial & Engineering Chemistry Research*, *41*, 3489.

Aziz, K., Ramesh, A. B., & Woo, P. T. (1987). Fourth SPE comparative solution project: comparison of steam injection simulators. *JPT*, *39*, 1576.

Cao, H. (2002). *Development of techniques for general purpose simulators* (Ph.D. thesis). Stanford University.

Christie, M., & Blunt, M. (2001). Tenth SPE comparative solution project: A comparison of upscaling techniques. *SPE Reservoir Evaluation and Engineering*, *4*, 308.

Coats, K. H. (1980). An equation of state compositional model. *Journal of Petroleum Science and Engineering*, *1*, 363.

Coats, K. H., Nielsen, R. L., Terhune, M. H., & Weber, A. G. (1967). Simulation of three-dimensional, two-phase flow in oil and gas reservoirs. *Transactions of the American Institute of Mining and Metallurgical Engineers*, *237*, 377.

Douglas, J., Peaceman, D. W., & Rachford, H. H. (1959). A method of calculating multi-dimensional immiscible displacement. *Transactions of the American Institute of Mining and Metallurgical Engineers*, *216*, 297.

Holderbaum, Th., & Gmehling, J. (1991). PSRK: A group-contribution equation of state based on UNIFAC. *Fluid Phase Equilibria*, *70*, 251.

Iranshahr, A., Voskov, D. V., & Tchelepi, H. A. (2010). Generalized negative-flash method for multiphase multicomponent systems. *Fluid Phase Equilibria*, *2*, 299.

Kiepe, J., Horstmann, S., Fischer, K., & Gmehling, J. (2004). Application of the PSRK model for systems containing strong electrolytes. *Industrial Engineering Chemistry Research*, *43*, 6607.

Lucia, A., Bonk, B. M., Waterman, R. R., & Roy, A. (2012). A multi-scale framework for multi-phase equilibrium flash. *Computers & Chemical Engineering*, *36*, 79.

Lucia, A., & Feng, Y. (2003). Multivariable terrain method. *AIChE Journal*, *49*, 2553.

Marcondes, F., Maliska, C. R., & Zambaldi, M. C. (2009). A comparative study of implicit and explicit methods using unstructured Voronoi meshes in petroleum reservoir simulation. *Journal of the Brazilian Society of Mechanical Sciences and Engineering*, *31*, 353.

Michelsen, M. L. (1982a). The isothermal flash problem. Part I. Stability. *Fluid Phase Equilibria*, *1*, 9.

Michelsen, M. L. (1982b). The isothermal flash problem. Part II. Phase-split calculation. *Fluid Phase Equilibria*, *1*, 9.

Odeh, A. S. (1981). Comparison of solutions to a three-dimensional black oil reservoir simulation problem. *JPT*, *33*, 13.

Ortega, J. M., & Rheinboldt, W. C. (1970). *Iterative solution of nonlinear equations in several variables*. Philadelphia, PA: SIAM.

Peaceman, D. W. (2000). *Fundamentals of numerical reservoir simulation*. Amsterdam, The Netherlands: Elsevier Scientific Publishing Co.

Peery, J. H., & Herron, E. H. (1969). Three-phase reservoir simulation. *Transactions of the American Institute of Mining and Metallurgical Engineers*, *246*, 211.

Peneloux, A., Rauzy, E., & Freze, R. (1982). A consistent correction for Redlich-Kwong-Soave volumes. *Fluid Phase Equilibria*, *8*, 7.

Peng, D. Y., & Robinson, D. B. (1976). A new two-constant equation of state. *Industrial Engineering Chemistry Fundamentals*, *15*, 59.

Price, H. S., & Coats, K. H. (1974). Direct methods in reservoir simulation. *Transactions of the American Institute of Mining and Metallurgical Engineers*, *257*, 295.

Reid, R., Prausnitz, J. M., & Poling, B. E. (1987). *The properties of gases and liquids* (4th ed.). New York, NY: McGraw-Hill Co.

Sandler, S. I. (1999). *Chemical and engineering thermodynamics* (3rd ed.). New York, NY: John Wiley & Sons, Inc.

Settari, A., & Aziz, K. (1974). A computer model for two-phase coning simulation. *Journal of Petroleum Science and Engineering*, *14*, 221.

Sheffield, M. (1969). Three-phase fluid flow including gravitational, viscous and capillary forces. *Transactions of the American Institute of Mining and Metallurgical Engineers*, *257*, 232.

Snyder, L. J. (1969). Two-phase reservoir flow calculations. *Journal of Petroleum Science and Engineering*, *9*, 170.

Soave, G. (1972). Equilibrium constants from a modified Redlich-Kwong equation of state. *Chemical Engineering Science*, *27*, 1197.

Todd, M. R., O'Dell, P. M., & Hirasaki, G. J. (1972). Methods for increased accuracy in numerical reservoir simulation. *Transactions of the American Institute of Mining and Metallurgical Engineers*, *253*, 515.

Trimble, R. H., & McDonald, A. E. (1976). A strongly coupled, implicit well coning model. In *Soc. Pet. Eng. 4th symposium on numerical simulation of reservoir performance* Los Angeles, CA, SPE Paper No. 5738.

Voskov, D., & Tchelepi, H. (2012). Comparison of nonlinear formulations for two-phase multi-component EOS-based simulation. *Journal of Petroleum Science and Engineering*, *82-83*, 101.

Voskov, D., & Tchelepi, H. (2009a). Compositional space parameterization: Theory and application for immiscible displacements. *Journal of Petroleum Science and Engineering*, *14*, 431.

Voskov, D., & Tchelepi, H. (2009b). Compositional space parameterization: Multi-contact miscible displacement and extension to multiple phases. *Journal of Petroleum Science and Engineering*, *14*, 441.

Voskov, D., & Zhou, Y. (2012). *Technical description of AD-GPRS*. Stanford, CA: Stanford University.

Whitson, C., & Michelsen, M. L. (1989). The negative flash. *Fluid Phase Equilibria*, *53*, 51.

Zaydullin, R., Voskov, D. V., & Tchelepi, H. A. (2013). Formulation and solution of compositional displacements in tie-simplex space. In *2013 SPE reservoir simulation symposium* Society of Petroleum Engineers, The Woodlands, TX.

Zhou, Y., Tchelepi, H. A., & Mallison, B. T. (2011). Automatic differentiation framework for compositional simulation on unstructured grids with multi-point discretization schemes. In *SPE reservoir simulation symposium* SPE141592, February 2011.